PROCEEDINGS OF SCIENCE

Results from proton-lead collisions

André Mischke*
Institute for Subatomic Physics, Department for Physics and Astronomy and EMMEϕ,
Faculty of Science, Utrecht University, Princetonplein 1, 3584 CS Utrecht, the Netherlands
E-mail: a.mischke@uu.nl

This contribution summarises recent measurements in small collision systems at the Large Hadron Collider (LHC), presented at the 2016 edition of the Annual Large Hadron Collider Physics conference. Three main probes are discussed, namely light flavour (strangeness) production, azimuthal angular correlations and jets, and open and hidden heavy-flavour production in proton-lead collisions.

Fourth Annual Large Hadron Collider Physics
13-18 June 2016
Lund, Sweden

*Speaker.

© Copyright owned by the author(s) under the terms of the Creative Commons Attribution-NonCommercial-NoDerivatives 4.0 International License (CC BY-NC-ND 4.0).

PoS(LHCP2016)019

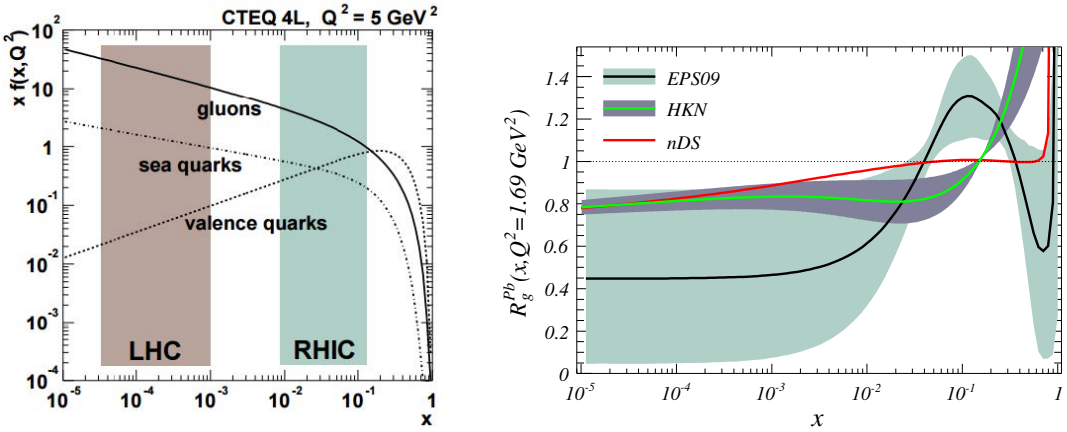

Figure 1: Bjorken-x distribution of gluons and quarks based on CTEQ 4L parton distribution functions (left panel) and the expected modification of the production cross section due to shadowing effects, shown as the ratio of bound over free proton gluon distributions and the virtuality $Q^2 = 1.69$ GeV^2 [7] (right panel).

1. Introduction

Proton-lead collisions allow the study of cold nuclear matter effects from the initial state such as

- Nuclear modification of the parton distribution functions (PDF) $\rightarrow$ shadowing at low Bjorken-x (dominant at the LHC);
- Gluon saturation from evolution equations (DGLAP and BFKL);
- k_{T} broadening and Cronin enhancement from multiple parton scatterings;
- Initial-state energy loss.

Final-state effects, if present, are expected to origin from energy loss and interactions between the final-state particles in a possible collective expansion. Initial-state effects, such as Cronin enhancement, nuclear shadowing and gluon saturation [1, 2, 3, 4], result in a modification of the production cross section [5] and provide crucial tests of perturbative Quantum-Chromodynamics (pQCD). They are important for the interpretation of the results from heavy-ions collisions [6]. Figure 1 illustrates the Bjorken-x distribution of gluons and quarks based on CTEQ 4L parton distribution functions (left panel) and the expected modification of the production cross section due to shadowing effects [7] (right panel).

2. Data sets

The data are obtained from collisions of a lead beam ($^{208}_{82}$Pb) with an energy of 1.58 TeV per nucleon and opposing proton beam with an energy of 4 TeV during the run-1 data taking in 2013. 13 bunches were circulating with about 10^{10} protons and 6×10^{7} Pb ions per bunch. The resulting centre-of-mass energy of the proton-lead system is $\sqrt{s_{\mathrm{NN}}} = 5.02$ TeV. Due to the energy asymmetry of the proton and lead colliding beams at the LHC, the centre-of-mass system of nucleon-nucleon collisions is shifted by $\Delta y = 0.465$ in the direction of the proton beam, with respect to the laboratory

PoS(LHCP2016)019

frame. Experimental data have been collected with two beam configurations (p–Pb and Pb–p) by inverting the orbits of the two particle species. The data reported in this contribution are obtained from the ATLAS, ALICE, CMS and LHCb experiments at the CERN-LHC [8]. Table 1 gives a summary of the recorded integrated luminosity of the different LHC experiments.

Experiment	Integrated luminosity
ALICE	$\approx 50\ \mu\text{b}^{-1}$
ATLAS	$\approx 30\ \text{nb}^{-1}$
CMS	$\approx 35\ \text{nb}^{-1}$
LHCb	$\approx 1.6\ \text{nb}^{-1}$

Table 1: Recorded integrated luminosity of the different LHC experiments.

3. Global event properties

Figure 2 (left panel) shows the transverse energy density per participant pair in pA and AA collisions as a function of the centre-of-mass energy [9]. The transverse energy density for 5.02 TeV proton-lead collisions of about 5.8 GeV is larger than the value for lead-lead collisions in the centrality class 70–80% and follows the linear raising trend observed at lower collision energies.
Femtoscopic measurements based on two-particle correlations image the spatio-temporal size of the particle emitting region. The ATLAS experiment performed identical-pion Hanbury Brown and Twiss (HBT) measurements using one- and three-dimensional correlation functions [10]. Pions are identified using dE/dx measured in the pixel detector. Correlation functions and the resulting HBT radii were studied as a function of pair momentum (k_{T}) and collision centrality. The product $R_{\mathrm{out}}R_{\mathrm{side}}R_{\mathrm{long}}$ scales linearly with the volume and is illustrated in Figure 2 (right panel) as a function of the averaged charged particle multiplicity for two different k_{T} regions. It exhibits a linear dependance, indicating a constant source density at the moment of freeze-out.

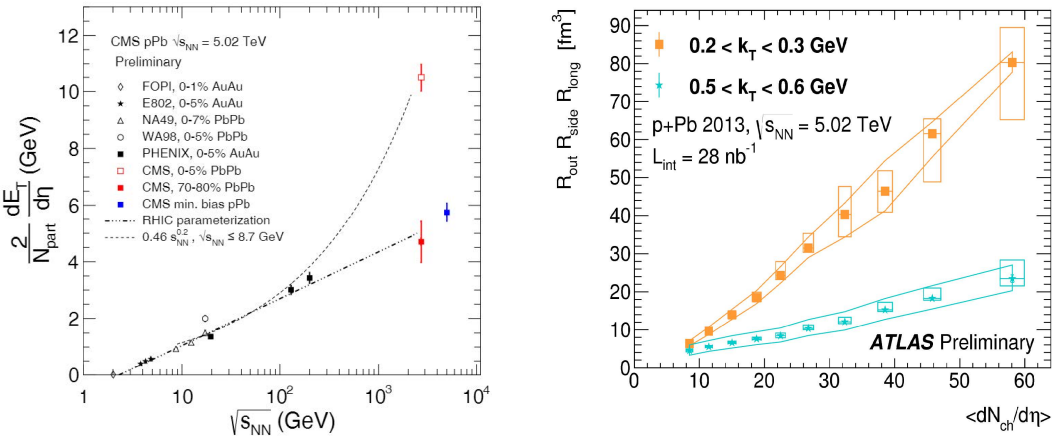

Figure 2: World data of the transverse energy density per participant pair in pA and AA collisions (left panel) [9] and the source volume versus charged particle density (right panel) [10].

PoS(LHCP2016)019

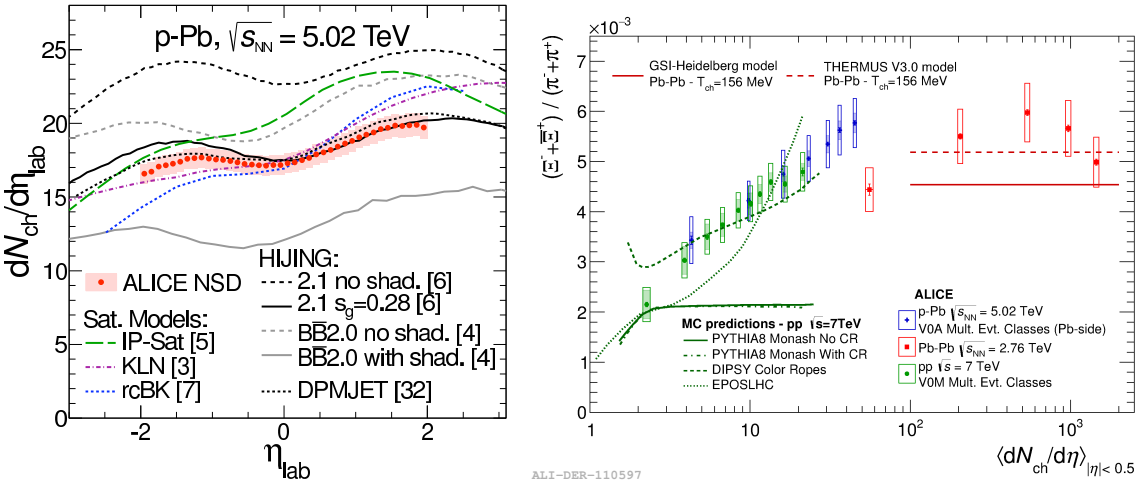

Figure 3: Left panel: Pseudorapidity density of charged particles in non-single diffractive (NSD) p–Pb collisions, measured by the ALICE experiment [11]. Right panel: $(\Xi^- + \Xi^+)/\pi^- + \pi^+)$ ratio as a function of charged particle multiplicity for the colliding systems pp, p–Pb and Pb–Pb. The ratios for the seven multiplicity classes in p–Pb data lie between the Minimum Bias pp and peripheral Pb–Pb results. The chemical equilibrium model predictions by the GSI-Heidelberg [13] and the THERMUS 2.3 [14] models and PYTHIA calculations with different tunes are represented by the coloured curves.

The ALICE experiment has measured the pseudorapidity density of charged particles over four units of pseudorapidity in non-single diffractive (NSD) p–Pb collisions (cf. in Figure 3, left panel). Most model predictions agree within 20% of the data [11]. However, saturation models rise too steeply with the pseudorapidity density, whereas pQCD-based Monte Carlo models such as HIJING and DPMJET describe the pseudorapidity density dependance.

The multi-strange baryon yields in lead-lead collisions have been shown to exhibit an enhancement relative to pp reactions. The Ξ and Ω production rates in proton-lead collisions have been measured with the ALICE detector as a function of transverse momentum [12]. The results cover the kinematic ranges 0.6 GeV/c $< p_{\mathrm{T}} <$ 7.2 GeV/c and 0.8 GeV/c $< p_{\mathrm{T}} <$ 5 GeV/c, for Ξ and Ω respectively, in the common rapidity interval -0.5 $< y_{\mathrm{CMS}} <$ 0. Multi-strange baryons have been identified by reconstructing their weak decays into charged particles. The p_{T} spectra are analysed as a function of event charged-particle multiplicity, which in p–Pb collisions ranges over one order of magnitude and lies between those observed in pp and Pb–Pb collisions. Figure 3 (right panel) shows the $(\Xi^- + \Xi^+)/\pi^- + \pi^+)$ ratio as a function of charged particle multiplicity for the colliding systems pp, p–Pb and Pb–Pb together with theoretical model calculations. The ratios for the seven multiplicity classes in p–Pb data lie between the Minimum Bias pp and peripheral Pb–Pb results. A similar multiplicity dependence in pp and p–Pb collisions as well as a continuous reduction of canonical suppression with increasing multiplicity is observed. Neither PYTHIA 6 nor 8 reproduce these data in any of the tunes tested. A statistical model is employed, which describes the change in the ratios with volume using a canonical suppression mechanism, in which the small volume causes a species-dependent relative reduction of hadron production. The calculations, in which the magnitude of the effect depends on the strangeness content, show good qualitative agreement with the data.

PoS(LHCP2016)019

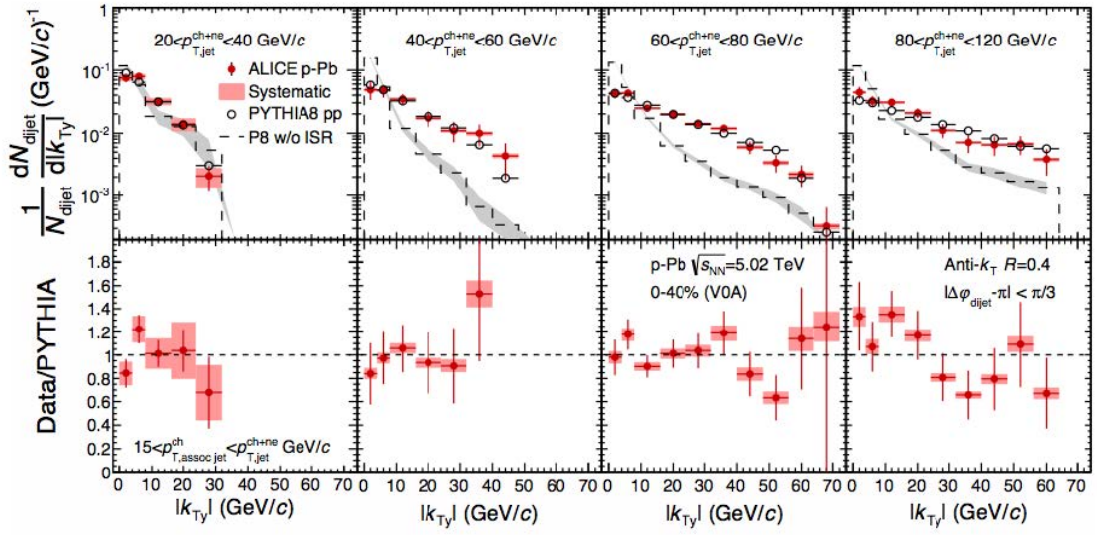

Figure 4: ALICE measurement [15] of the dijet $|k_{\mathrm{Ty}}|$ distributions in the most central 40% p–Pb collisions for different kinematic regions of the full jet ($p_{\mathrm{T,jet}}^{\mathrm{ch+ne}}$), compared to PYTHIA8 (tune 4C and K = 0.7) with and without initial state radiation. The lower panels show the ratio between the measurement and PYTHIA8 including initial state radiation.

4. Jets

The acoplanarity between full and charged jets has been studied by the ALICE Collaboration [15]. Jets are reconstructed from charged particles measured in the central tracking detectors and neutral energy deposited in the electromagnetic calorimeter. The transverse momentum of the full jet (clustered from charged and neutral constituents) and charged jet (clustered from charged particles only) is corrected event-by-event for the contribution of the underlying event, while corrections for underlying event fluctuations and finite detector resolution are applied on an inclusive basis. A projection of the dijet transverse momentum, $k_{\mathrm{Ty}} = p_{\mathrm{T,jet}}^{\mathrm{ch+ne}} \sin(\Delta\phi_{\mathrm{dijet}})$ with $\Delta\phi_{\mathrm{dijet}}$ the azimuthal angle between a full and charged jet and $p_{\mathrm{T,jet}}^{\mathrm{ch+ne}}$ the transverse momentum of the full jet, is used to study nuclear matter effects in p–Pb collisions. This observable is sensitive to the acoplanarity of dijet production and its potential modification in p–Pb collisions with respect to pp collisions. Measurements of the dijet k_{Ty} as a function of the transverse momentum of the full and recoil charged jet and the event multiplicity are depicted in Figure 4. No significant modification of k_{Ty} due to nuclear matter effects in p–Pb collisions with respect to the event multiplicity or a PYTHIA8 reference is observed. So, the p_{T} imbalance of jet correlations in Pb–Pb results are unlikely to originate from multiple scatterings in the nuclear target.

ALICE also investigated the azimuthal angular correlations between prompt D mesons and charged particles [16]. The near-side correlation peak is sensitive to characteristics of jet containing a D meson. Similar yields for p–Pb and pp were found. The data are well reproduced by PYTHIA calculations in all kinematic ranges.

PoS(LHCP2016)019

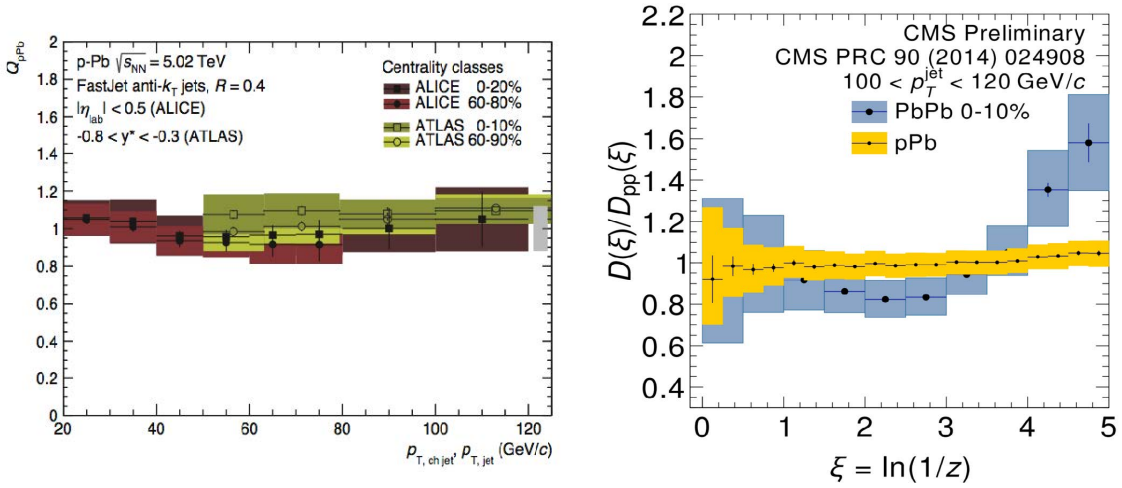

Figure 5: Left panel: Nuclear modification factor Q_{pPb} of charged jets measured by ALICE [17], compared to the nuclear modification factor for full jets as measured by ATLAS [18]. Note that the underlying parton p_{T} for fixed reconstructed jet p_{T} is higher in the case of charged jets. Right panel: Jet fragmentation function versus track momentum $\xi = \ln(p^{jet}/p^{track}_{long})$ [19].

Charged jets as a function of centrality were measured by ALICE [17], ATLAS [18] and CMS [19]. In ALICE, centrality classes are determined via the energy deposit in neutron calorimeters at zero degree, close to the beam direction, to minimise dynamical biases of the selection. The corresponding number of participants or binary nucleon–nucleon collisions is determined based on the particle production in the Pb-going rapidity region. Jets have been reconstructed in the central rapidity region from charged particles with the anti-k_{T} algorithm for resolution parameters $R = 0.2$ and $R = 0.4$ in the transverse momentum range 20 to 120 GeV/c. The reconstructed jet momentum and yields have been corrected for detector effects and underlying-event background.

The production yield has contributions from both initial- and final-state effects. These nuclear effects are typically quantified using the nuclear modification factor R_{AA}, where the production yield in nucleus-nucleus collisions is normalised by the yield in proton-proton reactions scaled by the number of binary collisions. Final state effects, such as radiative and collisional energy loss in the QGP matter, give an R_{AA} smaller than unity [20].

The centrality-dependent nuclear modification factor Q_{pPb} for charged and full jets, measured by the ALICE [17] and ATLAS Collaboration [18], respectively, is illustrated in the left panel of Figure 5. The jet production in p–Pb collisions is consistent with the production expected from binary scaling from pp collisions. The ratio of jet yields reconstructed with the two different resolution parameters is also independent of the centrality selection, demonstrating the absence of major modifications of the radial jet structure in the reported centrality classes.

The jet fragmentation function was measured by the CMS experiment [19] (cf. right panel of Figure 5) and is unmodified with respect to the interpolated pp reference. So, no cold nuclear matter effects are observed.

PoS(LHCP2016)019

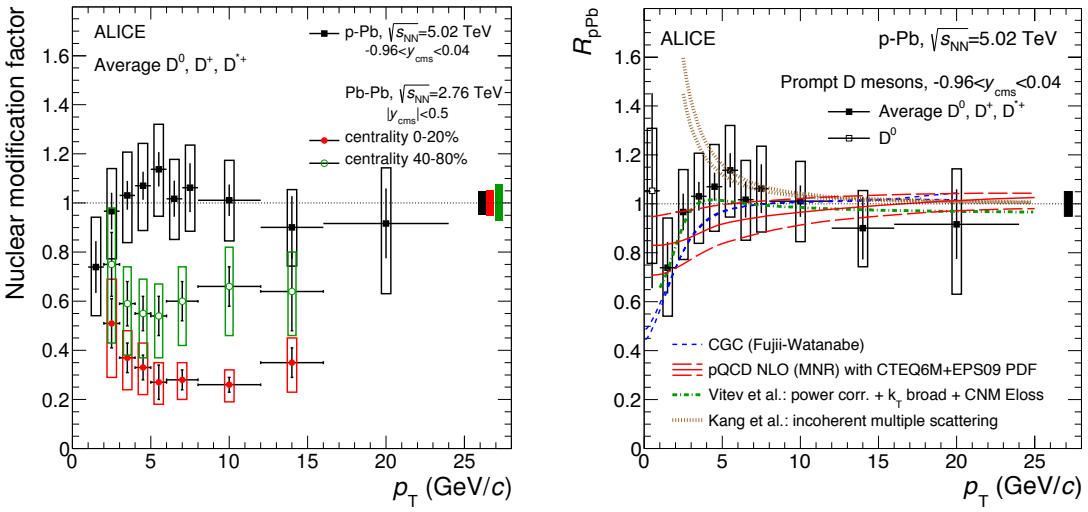

Figure 6: $R_{\rm AA}$ of the averaged prompt D mesons versus $p_{\rm T}$ for two different centralities in lead-lead collisions (red and green symbols) at $\sqrt{s_{\rm NN}}$ = 2.76 TeV [21] and in minimum bias proton-lead collisions (black symbols) at $\sqrt{s_{\rm NN}}$ = 5.02 TeV [23].

5. Open and hidden heavy flavour

Heavy-flavour particles, containing charm and beauty, are ideal probes of the conditions of the medium formed in nucleus-nucleus collisions at high energy since they experience the full space-time evolution of the expanding system. They propagate through the medium and lose energy due to gluon radiation and multiple collisions. The so-called "dead cone effect" is expected to reduce the radiative energy loss for heavy quarks compared to light quarks. By comparing the nuclear modification factor of charged pions ($R^{\pi^{\pm}}_{\rm AA}$), mostly originating from gluon fragmentation at this collision energy, with that of hadrons with charm $R^{\rm D}_{\rm AA}$ and beauty $R^{\rm B}_{\rm AA}$ the dependence of the energy loss on the parton nature (quark/gluon) and mass is investigated.

The D candidates are reconstructed in the hadronic decay channel using secondary vertexing. The left panel of Figure 6 illustrates the nuclear modification factor for prompt D mesons at mid-rapidity in lead-lead collisions at $\sqrt{s_{\rm NN}}$ = 2.76 TeV. The D meson yield for the most central events is strongly suppressed (by factor of ≈5 at around 10 GeV/c). Energy loss models currently describe the observed suppression at high transverse momentum reasonably well [21] whereas the description at low transverse momentum ($\leq$ 2 GeV/c) is more challenging. The D meson yields are suppressed at the same level as observed for light-quark hadrons, which was not expected due to the dead-cone and colour-charge effects. Measurements based on non-prompt J/ψ production [22] provide first indications for a smaller energy loss for beauty compared to charm.

To quantitatively understand the heavy-ion data in terms of energy loss, it is important to disentangle the hot nuclear matter from cold nuclear matter effects. The latter initial-state effects can be investigated in proton-lead collisions. The $R_{\rm pPb}$ of prompt D mesons in p–Pb at $\sqrt{s_{\rm NN}}$ = 5.02 TeV [23] is shown in Fig. 6 (left panel) and is compatible with unity within systematic uncertainties over the full $p_{\rm T}$ range. Thus, the strong suppression of the heavy-flavour hadron yield observed in central Pb-Pb collisions is indeed a final-state effect and arising from

PoS(LHCP2016)019

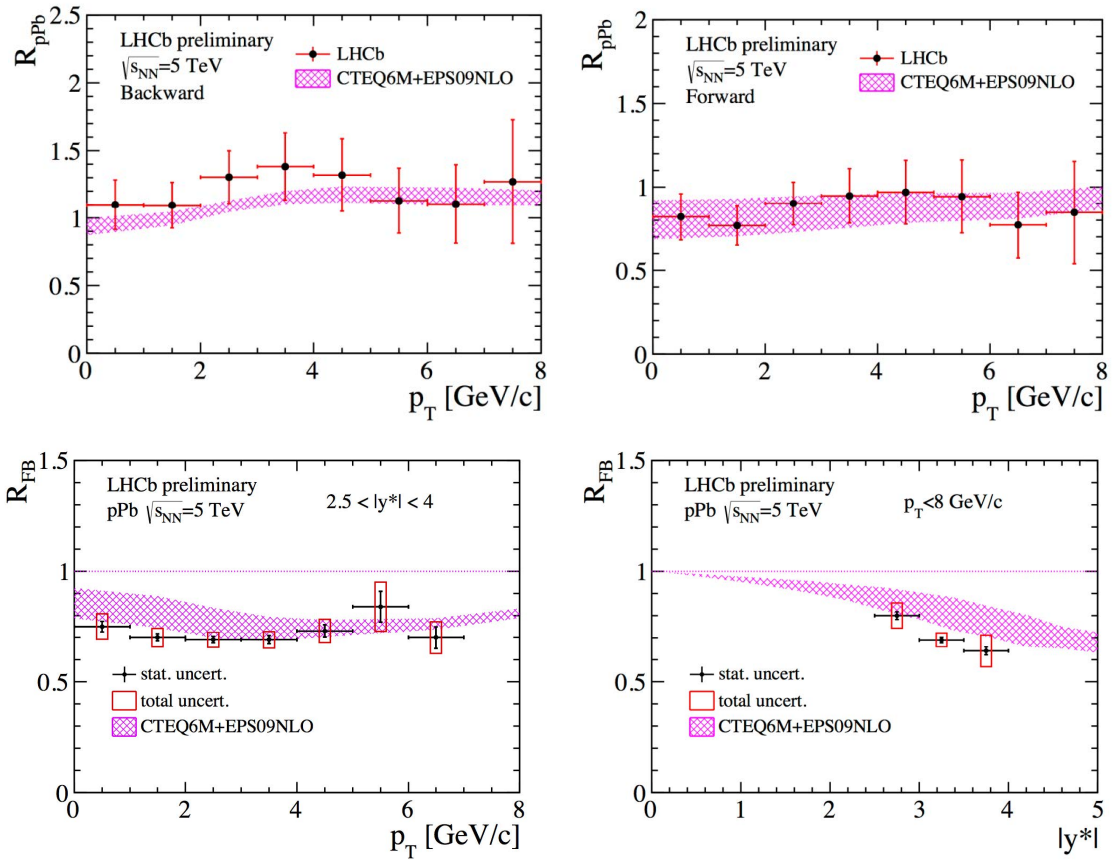

Figure 7: Transverse momentum dependance of the nuclear modification factor R_{pPb} in the (upper left panel) backward data and forward rapidities (upper right panel) [25]. Forward-backward production ratio R_{FB} as a function of (lower left panel) p_{T} integrated over $2.5 < |y^*| < 4.0$ and as a function of y integrated over $p_{\mathrm{T}} < 8$ GeV/c (lower right panel). The uncertainty is the quadratic sum of the statistical and systematic components.

the QCD matter. The data are consistent with predictions from shadowing [7] and color glass models [24], which consider cold nuclear matter effects only. The data disfavour a suppression larger than 15% at high p_{T}, which rule out models with a small plasma phase (e.g. POWLANG).

The LHCb experiment has measured prompt D^0 meson production cross section at forward ($2.5 < y < 4.0$, proton going side) and backward rapidities ($-2.5 > y > -4.0$, lead going side) [25]. The upper panels in Figure 7 depict the nuclear modification factor R_{pPb} as a function of p_{T} in the (left) backward data and (right) forward data, integrated over the common rapidity range $2.5 < |y^*| < 4.0$. Open charm production is well described by pQCD calculations including nuclear PDF's. However, a large asymmetry in the forward-backward production is observed, suggesting a strong cold nuclear matter effect and the data are slightly more suppressed at high-y^* (cf. lower panels in Figure 7).

The nuclear modification factor of fully reconstructed B mesons in the exclusive hadronic decay channel $B^+ \to J/\Psi K^+ \to \mu^+\mu^- K^+$ at mid-rapidity ($y_{\mathrm{lab}} < 2.4$) and $10 < p_{\mathrm{T}} < 60$ GeV/c was measured by the CMS Collaboration [26] (cf. Figure 8). No indication of significant cold nuclear matter

PoS(LHCP2016)019

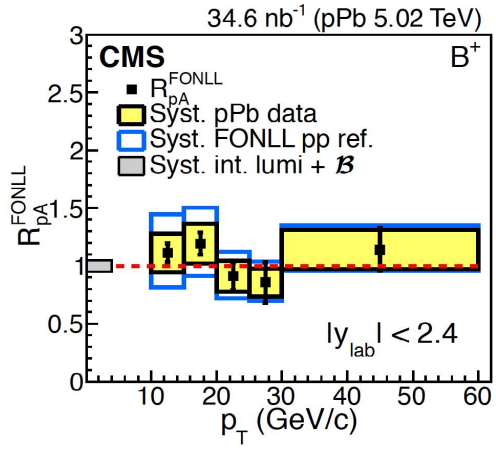

Figure 8: The nuclear modification factor $R_{\mathrm{pA}}^{\mathrm{FONLL}}$ of B^+ mesons as a function of p_{T} [26]. The statistical and systematic uncertainties on the p–Pb data are shown as bars and yellow boxes around the data points, respectively. The systematic uncertainties from the FONLL predictions are plotted separately as open blue boxes. The global systematic uncertainties are shown as full grey boxes at unity.

effects on beauty production were found, considering the statistical and systematical uncertainties, when compared to pp FONLL calculations scaled by the number of incoherent nucleon-nucleon collisions. These results provide a baseline for the study of in-medium beauty-quark energy loss in lead-lead collisions.

The CMS experiment measured charm [27] and beauty jets in proton-lead collisions [28]. Charm jets are identified by requiring a secondary vertex comprised of three or more charged tracks that are significantly displaced from the primary vertex. A variant of the secondary vertex mass is used to extract the relative contributions of jet flavours. Jets from b quark fragmentation are found by exploiting the long lifetime of hadrons containing a b quark through tagging methods using distributions of the secondary vertex mass and displacement. The extracted cross sections for b jets

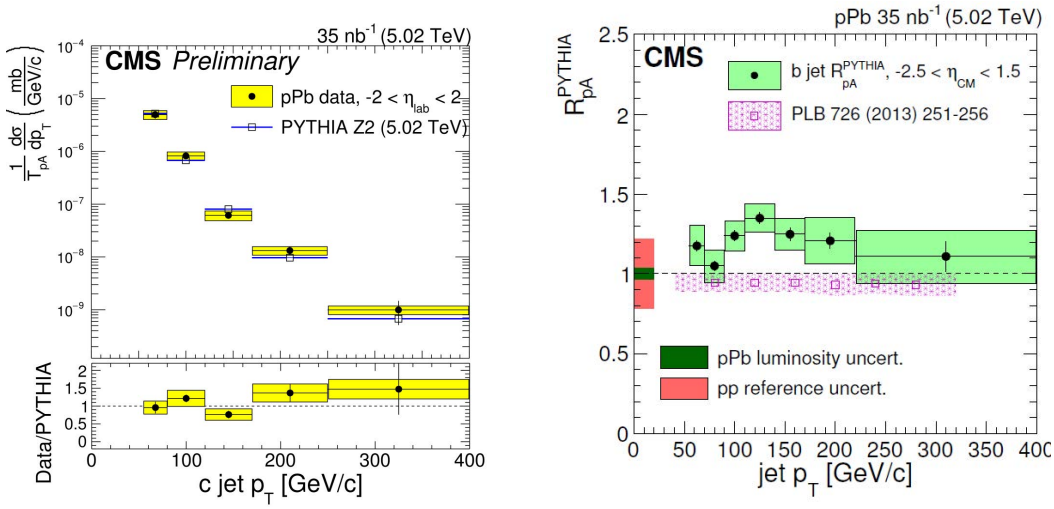

Figure 9: Charm-jet p_{T} differential cross section consistent compared with PYTHIA calculations [27] (left panel) and inclusive beauty jet R_{pPb} versus p_{T} [28] (right panel).

PoS(LHCP2016)019

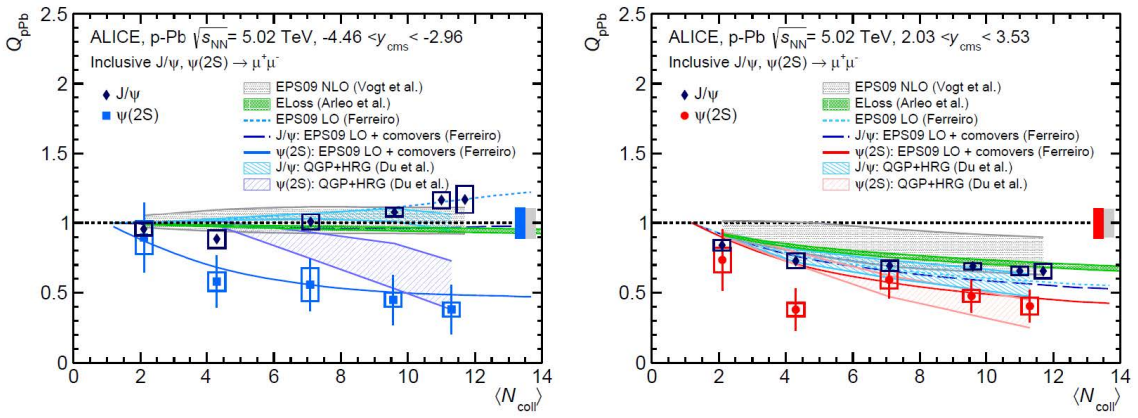

Figure 10: J/ψ and Ψ(2S) nuclear modification factors Q_{pPb} as a function of number of colliding nucleons for the backward (left panel) and forward (right panel) rapidity regions and compared to theoretical model calculations [30].

are scaled by the effective number of nucleon-nucleon collisions and are compared to a reference obtained from PYTHIA simulations of pp collisions. The charm-jet p_{T} differential cross section, shown in Figure 9 (left panel), is consistent with PYTHIA calculations. The inclusive beauty jet R_{pPb} is in agreement with the pp reference (cf. right panel of Figure 9).

In summary we can conclude that no significant cold nuclear matter effects are observed on open heavy-flavour production at high transverse momentum.

The nuclear modification factor of J/ψ and Ψ(2S) was studied in the dimuon final states by the LHCb and ALICE Collaboration. In LHCb [29], the measurement is performed using Ψ(2S) mesons with transverse momentum less than 14 GeV/c and rapidity y in the ranges $1.5 < y < 4.0$ and $-5.0 < y < -2.5$ in the nucleon-nucleon centre-of-mass system. The forward-backward production ratio and the nuclear modification factor are determined for Ψ(2S) mesons. The forward-backward production ratio R_{FB} is determined separately for prompt Ψ(2S) mesons and those from b-hadron decays. These results show agreement within uncertainties with available theoretical predictions. The nuclear modification factor R_{pPb} is also determined separately for prompt Ψ (2S) mesons and Ψ(2S) from beauty decays. These results show that prompt Ψ(2S) mesons are significantly more suppressed than prompt J/ψ mesons in the backward region. The results are not well described by theoretical predictions based on shadowing and energy loss mechanisms.

The inclusive production of the J/ψ and Ψ(2S) charmonium states was studied with the ALICE detector as a function of centrality in proton-lead collisions [30]. The measurement was performed in the centre of mass rapidity ranges $-4.46 < y_{\mathrm{cms}} < -2.96$ and $2.03 < y_{\mathrm{cms}} < 3.53$ down to zero transverse momentum. The J/ψ and Ψ(2S) nuclear modification factors Q_{pPb} as a function of number of colliding nucleons (N_{coll}) for the backward (left panel) and forward (right panel) rapidity regions is illustrated in Figure 10. The results show a large multiplicity dependent suppression of Ψ(2S) production relative to the J/ψ at backward (negative) rapidity, corresponding to the flight direction of the lead-nucleus, while at forward (positive) rapidity the suppressions of the two states are comparable. Effects such as shadowing or energy loss are enough to explain the J/ψ behaviour,

PoS(LHCP2016)019

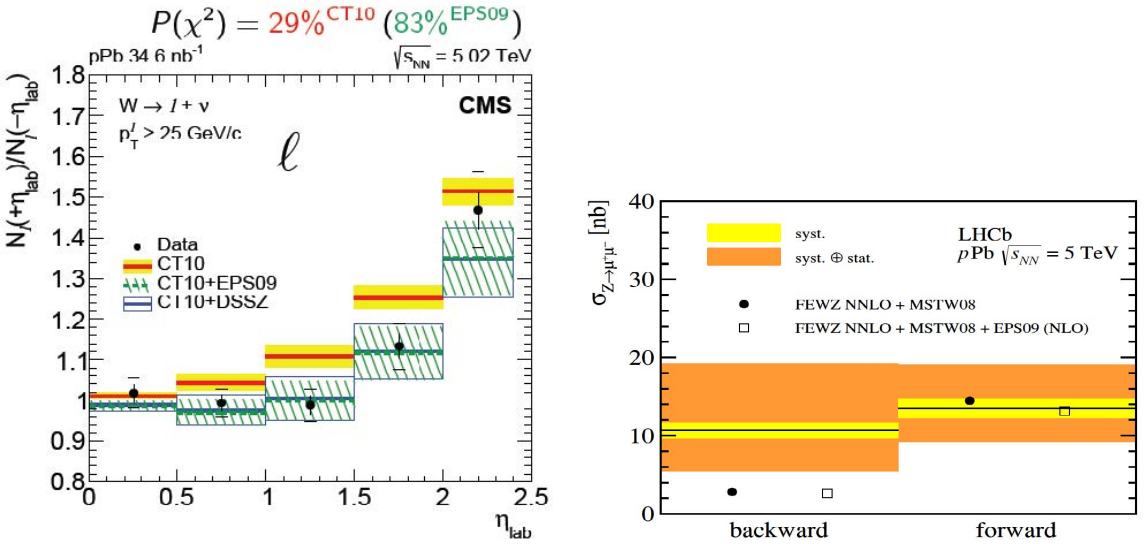

Figure 11: Left panel: CMS measurement of the forward-backward asymmetry of charge-summed W bosons as a function of the lepton pseudorapidity [32]. Error bars represent the statistical uncertainties, while brackets show statistical and systematic uncertainties summed in quadrature. Theoretical predictions assuming both modified (CT10+EPS09, dashed green line) and unmodified nuclear PDF's (CT10, solid red line) are also shown, with their uncertainty bands. Right panel: $Z \to \mu^+\mu^-$ production cross section measured by LHCb [35] and compared with NNLO FEWZ calculations with and without nuclear PDFs.

while additional mechanisms are needed to describe the Ψ(2S) suppression. Theoretical models that include final state interactions are able to reproduce such a suppression. Processes occurring at later times (final-state effects), such as the break-up through interactions with co-moving hadrons and dissociation of fully-formed resonance in nuclear matter, might explain the observed Ψ(2S) suppression.

6. W and Z production

The CMS experiment performed the measurement of W boson production in proton-lead collisions for bosons decaying into a muon or electron and a neutrino [32]. The W boson differential cross sections, lepton charge asymmetry, and forward-backward asymmetries are measured for leptons of transverse momentum exceeding 25 GeV/c, and as a function of the lepton pseudorapidity in the $\eta_{\rm lab} < 2.4$ range. The forward-backward asymmetries, illustrated in the left panel of Figure 11, show a deviation from unmodified parton distribution functions and urge the need for including W boson data in nuclear parton distribution global fits.

The ATLAS Collaboration has measured the inclusive production of Z bosons via their decays into electron and muon pairs [33]. It is found to be slightly higher than predictions based on perturbative QCD calculations. Disregarding the difference in overall normalisation, the shapes of the rapidity and x-dependent cross sections are somewhat better described by models that include nuclear modification of the nuclear PDF compared to those that do not, although models without nuclear modification are not excluded.

PoS(LHCP2016)019

This finding is supported by the measurement of the CMS experiment via the electron and muon decay channels [34] where a forward-backward asymmetry was observed that suggests the presence of nuclear effects at large rapidities.
The production of Z bosons was also studied by the LHCb Collaboration in the forward and backward directions [35], through the reconstruction from pairs of oppositely charged muons with pseudo-rapidities between 2.0 and 4.5 and transverse momenta above 20 GeV/c. The invariant dimuon mass is restricted to the range 60–120 GeV/c^2. The Z production cross section, shown in the right panel of Figure 11, was found to be in agreement with predictions, although the one in the backward direction appears to be higher than predictions. The forward-backward ratio R_{FB} in the Z rapidity interval $2.5 < |y| < 4.0$ in the centre-of-mass frame is found to be lower than expectations, and corresponds to a 2.2σ deviation from $R_{\mathrm{FB}} = 1$. The statistical uncertainties yet prevent distinction among different nuclear parton distribution functions.

7. Summary

The proton-lead programme at the CERN-LHC allowed studying cold-nuclear effects such as shadowing and gluon saturation. Recent results on the measurement of light and heavy-flavour production and jets were presented.
The strange hadron results give a clear indication for a continuous reduction of canonical suppression with increasing multiplicity. Jet fragmentation exhibits no modification in proton-lead collisions. No significant modification is observed for the production of prompt D mesons, B mesons, charm and beauty jets. The J/ψ measurements are consistent with shadowing effects, whereas the Ψ(2S) is not described by (anti)shadowing and energy loss models only. So overall we can say that no evidence is observed for substantial modifications due to cold nuclear matter effects (except for quarkonia). Electroweak bosons favour the modification of nuclear parton distribution functions.
Furthermore, indication for collective-like behaviour in small systems were found, reminiscent of that observed in lead-lead collisions. It is not clear whether it originates from final-state effects in proton-lead collisions. The origin of this new phenomenon, called the "long-range correlation in pseudorapidity", is not fully understood yet and will further be investigated with the run-2 p–Pb data taking at 5 and 8 TeV collision energy in 2016. The increase of the interaction rate for the LHC run-3 after the second long shutdown in 2019/20 will require a significant upgrade of the experiments to improve substantially the current performances, especially for the measurements of heavy-flavour particles and jets.

Acknowledgments

Sincerest thanks to the ALICE, ATLAS, CMS and LHCb Collaboration for providing the data and the LHC accelerator team. This work was supported by the Netherlands Organisation for Scientific Research (project number: 680-47-232) and the Dutch Foundation for Fundamental Research (project numbers: 12PR3083).

PoS(LHCP2016)019

References

[1] C.A. Salgado et al., J. Phys. G 39, 015010 (2012) [arXiv:1105.3919].

[2] J.W. Cronin, H.J. Frisch, M.J. Shochet, J.P. Boymond, P.A. Piroue and R.L. Sumner, Phys. Rev. D 11, 3105 (1975).

[3] A. Accardi, hep-ph/0212148.

[4] R.C. Hwa and C. Yang, Phys. Rev. Lett. 93, 082302 (2004).

[5] K. Mueller, these proceedings.

[6] C. Loizides, Nuclear Physics A 956 (2016) (arXiv:1602.09138).

[7] K.J. Eskola, H. Paukkunen, C.A. Salgado, JHEP 0904, 65 (2009)

[8] A. Breskin and R. Voss, JINST 3, S08001-S08007 (2008).

[9] CMS Collaboration, CMS-HIN-14-014.

[10] ATLAS Collaboration, ATLAS-CONF-2015-054.

[11] ALICE Collaboration, Phys. Rev. Lett. 110, 032301 (2013).

[12] ALICE Collaboration, Phys. Lett. B 758 (2016) 389 and Phys. Lett. B 728 (2014) 25.

[13] A. Andronic, P. Braun-Munzinger, and J. Stachel, Phys. Lett. B 673 (2009) 142.

[14] S. Wheaton, J. Cleymans, and M. Hauer, Computer Physics Communications 180 (2009) 84.

[15] ALICE Collaboration, Phys. Lett. B 746 (2015) 385.

[16] ALICE Collaboration, submitted to EPJC (arXiv:1605.06963).

[17] ALICE Collaboration, Eur. Phys. J. C76, 271 (2016) and Phys. Rev. C91, 064905 (2015).

[18] ATLAS Collaboration, Phys. Lett. B 748, 392 (2015).

[19] CMS Collaboration, CMS-PAS-HIN-15-004

[20] R. Baier et al., Nucl. Phys. B 483, 291 (1997).

[21] B. Abelev et al. (ALICE Coll.), JHEP 09, 112 (2012).

[22] C. Mironov et al. (CMS Coll.), Nucl. Phys. A 904-905, 194c (2013).

[23] B. Abelev et al. (ALICE Coll.), submitted to JHEP (arXiv:1605.07569) and Phys. Rev. Lett. 113, 232301 (2014)

[24] H. Fujii and K. Watanabe, Nucl Phys. A 920, 78 (2013).

[25] LHCb Collaboration, LHCb-CONF-2016-003.

[26] CMS Collaboration, Phys. Rev. Lett. 116 (2016) 032301.

[27] CMS Collaboration, CMS-PAS-HIN-15-012.

[28] CMS Collaboration, Phys. Lett. B 754 (2016) 59.

[29] LHCb Collaboration, JHEP 1402 (2014) 072 and JHEP 1603 (2016) 133.

[30] ALICE Collaboration, JHEP 1402 (2014) 073 and JHEP 1412 (2014) 073.

[31] ALICE Collaboration, JHEP 1606 (2016) 050 and JHEP 1511 (2015) 127.

PoS(LHCP2016)019

[32] CMS Collaboration, Phys. Lett. B 750 (2015) 565.

[33] ATLAS Collaboration, Phys. Rev. C 92, 044915 (2015).

[34] CMS Collaboration, Phys. Lett. B 759, 36 (2016).

[35] LHCb Collaboration, JHEP 1409, 030 (2014).

PoS(LHCP2016)019